Hindawi
Advances in Civil Engineering
Volume 2023, Article ID 8819066, 18 pages
https://doi.org/10.1155/2023/8819066

Research Article

Study on Control of Cumulative Risk for Submarine Tunnel Shield Construction

Kang Meng, Mingda Li, and Jing Zhou

State Key Laboratory of Coastal and Offshore Engineering, Dalian University of Technology, Dalian, China

Correspondence should be addressed to Kang Meng; mengkangoffice@mail.dlut.edu.cn

Received 27 December 2022; Revised 7 February 2023; Accepted 15 April 2023; Published 24 April 2023

Academic Editor: Yi Zhang

Researching the control of cumulative risk for submarine tunnel shield construction is of great significance for improving risk management capability. Firstly, the concepts of cumulative risk, fragility, and the theory of system dynamics (SD) are introduced. Secondly, the risk conduction network is established, and the risk conduction mechanism based on fragility is analyzed. Then, the cumulative risk control model is established by SD. Finally, Dalian Metro Line 5 Cross-sea Large Diameter Shield Construction Project is used to verify the model. Simulations of cumulative risk with and without control measures are compared, and the result is in line with objective facts. The correctness and effectiveness of the model are verified.

1. Introduction

In the engineering construction field, risk research was first applied and developed in structural engineering. The tunnel construction risk research started late but developed rapidly. The representative figure of tunnel construction risk research is the American scholar Einstein. He was the first to introduce risk management ideas into tunnel construction and made remarkable contributions. He has compiled many academic papers and scientific works on tunnel risk identification, analysis, evaluation, and control methods [1–4]. According to the potential safety problems in the tunnel construction, the reliability analysis method was introduced by Isaksson to select construction schemes for shield tunnel and improve construction quality [5]. Chapman thoroughly studied the risk management in the tunnel construction and designed an expert system management software for the first time [6]. Stuzk et al. learned from the risk management experience of the Stockholm Ring tunnel project in Sweden, explored the risk management strategies and methods during the construction of large-scale underground tunnel projects in depth, and put forward some constructive suggestions and analytical theories [7]. For the first time, Japanese scholar Sato Hisashi systematically analyzed the types and characteristics of tunnel engineering risks based on a large number of statistical data on tunnel engineering safety accidents [8]. The Guide to Risk Management of Tunnel Engineering published by the International Tunnel Association (ITA) in International Tunnel has set a milestone for the risk research of tunnels and underground engineering, marking a new stage of the research [9]. In addition, many qualitative and quantitative methods or theories have been applied to tunnel construction risk research, such as Bayesian network, fault tree analysis, and analytic hierarchy process [10, 11].

With the development of the economy and society and the progress of science and technology, tunnels are gradually used to connect the two sides of the strait or the bay. Due to its high safety under severe weather conditions, strong seismic performance, and combat readiness, the submarine tunnel has received extensive attention and favor. However, the complex geological environment, large engineering quantities, high technical difficulty and strong concealment, and other undesirable characteristics make the construction accidents occur from time to time, such as the gushing accidents of the Seikan Tunnel in Japan, the fire accident of the Channel Tunnel, and the rupture of the tunnel of the Hong Kong-Zhuhai-Macao Bridge [12–14]. These have attracted great attention from scholars in the field of risk management. Duddeck made a risk assessment of the

submarine tunnel project for the first time and applied his research theory to guide engineering practice [15]. Rich experiences have been gained in Norway from constructing many submarine tunnels in its special geographical environment, and the "Norwegian submarine tunnel concept" was proposed. The concept was believed that the risk of submarine tunnel shield construction mainly came from two aspects: surrounding rock conditions and construction countermeasures [16]. Wang, an academician of the Chinese Academy of Engineering, conducted a systematic analysis of the design, construction, and operation of the submarine tunnel and put forward risk management countermeasures at various stages [17].

Cumulative risk belongs to the research category of psychology and toxicology. For example, Xiong et al. have conducted a systematic study on the adverse effects of cumulative risk on the mental health of adolescents. Compared with single factors, it is more meaningful to study the impact of cumulative risk on mental health [18]. In toxicology, Chang believes that it is more meaningful to take the food safety risk caused by the cumulative effect of food additives as the assessment object [19]. In recent years, cumulative risk can also be occasionally found and applied in the fields of insurance and the power industry [20, 21].

To sum up, scholars have conducted some research on the theory and application of risk management in tunnel construction and put forward a variety of solutions for risk identification, risk assessment, and risk sharing during the tunnel construction. Simultaneously, they recognized the important role of risk management in the submarine tunnel construction. However, there are still the following shortcomings: ① weak pertinence and lack of special research on the risk of the submarine tunnel; ② focusing on static research. Most studies ignore the variability of risks and lack dynamic assessment of risks; ③ no proposal for risk control of submarine tunnel construction; ④cumulative risk has not been used in risk management of tunnel construction.

In terms of these problems, this paper targets the construction process of the submarine tunnel shield as the research object and proposes a risk control model based on its characteristics, aiming to improve the risk management ability of submarine tunnel shield construction. One of the main contributions of this research is to introduce the concept of cumulative risk into the management of submarine tunnel shield construction and to establish a control model of cumulative risk by applying SD. In the meantime, the fragility is assessed and adjusted to improve the system's ability to resist risks, providing a solution for controlling the risk of submarine tunnel shield construction. As far as we know, this is the first time that cumulative risk has been applied to the risk management of engineering construction projects, demonstrating the process in which risk is conducted during the submarine tunnel shield construction and is effectively controlled under measures to reduce the fragility.

The paper has been organized in the following way: in Section 2, the concepts of cumulative risk, fragility, and the theoretical basis of SD are introduced. In Section 3, based on the research of risk conduction network and risk conduction mechanism, a control model of cumulative risk is constructed. In Section 4, the proposed model is illustrated by Dalian Metro Line 5 Cross-sea Large Diameter Shield Construction Project and the application results of the model are discussed. Conclusions are drawn in Section 5.

2. Background and Preliminaries

2.1. Risk of Submarine Tunnel Shield Construction. The environment of submarine tunnel shield construction is under the seabed of tens of meters or even hundreds of meters, and it is often faced with the challenges of water-rich surrounding rock, weathering trough, karst cave, and other adverse geological conditions. Therefore, the difficulty of submarine tunnel shield construction is far higher than that of general engineering projects. It is necessary to overcome the difficulties of high equipment requirements, long-distance tunneling, and high-water seepage pressure. At the same time, the particularity of the geological environment and the limitations of the survey technology put forward the requirements of high strain capacity. The uncertainty of the actual geological conditions and other emergencies are also risks that need special attention in the submarine tunnel shield construction.

In general, the risk of submarine tunnel shield construction refers to the adverse effects of risk factors throughout the whole process of submarine tunnel shield construction. Specifically, these factors cause casualties of construction personnel, damage to materials and equipment, damage to the main body of the tunnel, time delay, economic losses, and other consequences. The risk of submarine tunnel shield construction has the characteristics of objectivity, diversity, stage, dynamicity, and conductivity.

2.2. Cumulative Risk. The concepts of cumulative risk in toxicology, environmental science, and psychology are introduced hereafter. Toxicology proposes that people are exposed to multiple pollutants through multiple channels every day. The total exposure caused by two or more pollutants through different channels and media is called cumulative exposure, and the health risk caused by cumulative exposure is called cumulative risk [22]. Environmental Science defines cumulative risk as the combined risk from comprehensive exposure including physical, chemical, and biological pressure sources [23]. Psychology emphasizes the development of individuals nested in a series of environmental systems that influence each other. The risk factors of each system co-occur and accumulate with the growth of individuals to form cumulative ecological risks. After reaching the threshold, it will cause mental illness [24].

Cumulative risk in different research fields is given different connotations, but they are characterized by objectivity, diversity, long-term nature, variability, and conductivity. Similarly, the submarine shield tunnel project has a large amount of work, long construction period, complex geological environment, and high technical difficulty. These expose the process of submarine tunnel shield construction to a variety of risk factors for a long time, and

various risk factors always co-occur and work together. Obviously, the risk of submarine tunnel shield construction also shows similar characteristics to the cumulative risk.

Inspired by the coincidence of similar characteristics, the concept of cumulative risk is introduced into the risk management of submarine tunnel shield construction: during the submarine tunnel shield construction, it is always exposed to the system and nonsystem risk factors. As the construction progresses, the risk factors interact with each other and produce cumulative effects, which is called cumulative risk (CR).

2.3. Fragility. Fragility was first used in structural engineering to describe the difficulty of structural failure [25]. To date, fragility has become a new area of research focus, which has been given different connotations and is widely used in financial systems, ecosystems, industrial systems, and information security systems. Even so, the fragility in each system still retains the characteristics of internality, dynamics, and controllability. Based on the above-mentioned characteristics, fragility is introduced into the study of CR. The fragility of submarine tunnel shield construction is defined as the ability to resist the attack of risk factors (R) determined by the internal factors of the submarine tunnel shield construction system. The higher the fragility value is, the weaker the system's ability to resist risk is.

2.4. Introduction to SD. SD is a discipline created in 1956 by Professor Forrester of the Massachusetts Institute of Technology. It is based on system theory, cybernetics, and information theory and aims to study complex information feedback systems. SD takes computer simulation technology as the main method. It studies the structure of complex systems quantitatively and qualitatively from the internal causality structure of the system, especially dealing with complex time-varying systems with multivariables, high order, and nonlinearity [26]. Therefore, SD can be based on simulation experiments to investigate the system's response and dynamic changes under different parameter inputs or different strategies so that decision-makers can try different scenarios and observe simulation results.

SD emphasizes that system behavior is determined by the causal feedback mechanism inside the system. The causal loop diagram can be used to express the direct causality and feedback loops of various parts of the system. The causal loop diagram is composed of links. The link represents the causal relationship between variables. It is represented by an arrow marked with a sign. The tail of the arrow connects to the independent variable, and the arrow connects to the dependent variable. "+" indicates that the dependent variable changes in the same direction with the independent variable, and "−" indicates that the dependent variable changes in the opposite direction with the independent variable. A closed loop formed by connecting multiple causal chains at the beginning and end is called a feedback loop. The loop also has positive and negative polarities. The loop contains an even number of negative links, and its polarity is positive, as shown in Figure 1(a). If the loop contains an odd number of negative links, its polarity is negative, as shown in Figure 1(b).

The flow graph can intuitively describe the cumulative effect that affects the dynamic performance of the feedback system. Its basic elements include variables and flows. The flows are divided into the material flow and information flow. The variables are mainly as follows. ① *Level Variable*. It is the variable that ultimately determines the behavior of the system. As time goes by, the current value is equal to the past value plus the amount of change in this period of time. ② *Rate Variable*. It reflects the speed of accumulating variable input or output. ③ *Auxiliary Variable*. It is obtained by other variables in the system, and the current value and the past value are independent of each other. ④ *Exogenous Variable*. It changes over time, but it is not caused by other variables in the system. ⑤ *Constant Variable*. It is a constant value that does not change with time. The variables and flows are expressed in different symbols, as shown in Figure 2.

3. Model Construction

This section may be divided into subheadings. It should provide a concise and precise description of the experimental results, their interpretation as well as the experimental conclusions that can be drawn.

3.1. Risk Conduction Network Construction

3.1.1. Identification of Risk Factors. In this paper, 16 extremely relevant papers were studied. According to the principles of completeness, rationality, and applicability, 33 risk factors (R_i, $i = 1, 2, \ldots, 33$) that are common in submarine tunnel shield construction were screened out. They were divided into five types (R_X, $X = S, P, L, N, R$): systematic risk factors (R_S), preparing stage risk factors (R_P), launching stage risk factors (R_L), normal tunnelling stage risk factors (R_N), and receiving stage risk factors (R_R). R_P, R_L, R_N, and R_R are nonsystem risk factors, as shown in Table 1.

3.1.2. Risk Conduction Theory. With reference to the energy release theory in risk research, risk conduction is defined as the risk energy released by the risk issuer, under the promotion or hindrance of the risk conduction carrier, forms a process of risk flow along the risk conduction path to reach the risk receiver. The 33 risk factors are set as risk variables (R_i) in turn, and the variable of risk flow (R_X) is introduced. There is a causal relationship between the risk variables in the same stage, and the risk flow of this stage is formed. R_S, R_P, R_L, R_N, and R_R, respectively, represent the systematic risk flow, the risk flow in the preparing stage, the risk flow in the launching stage, the risk flow in the normal tunnelling stage, and the risk flow in the receiving stage. According to the sequence of time, it is conducted from the previous stage to all subsequent stages, and the systemic risk is conducted at each stage of the nonsystematic risk. As a result, all risk flows will eventually converge through conduction to form CR, as shown in Figure 3. According to graph theory, the risk

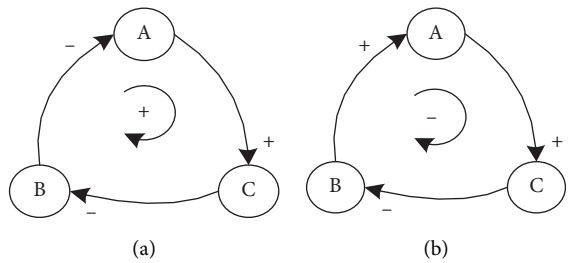

Figure 1: Causal loop diagram.

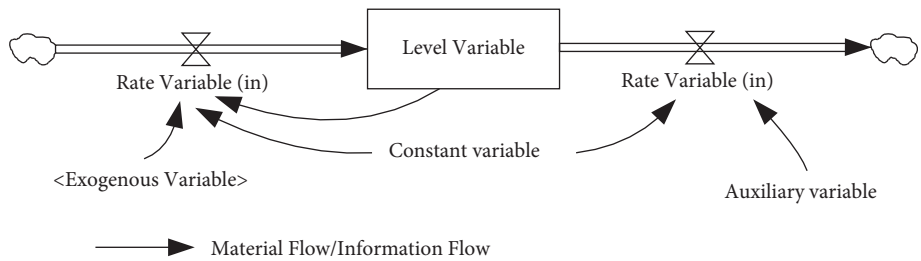

Figure 2: Flow graph of SD.

Table 1: Risk factors.

R_X	R_i
R_S	Policy (R_1)
	Public opposition (R_2)
	Force majeure (R_3)
	Contract (R_4)
	Construction term (R_5)
R_P	Instability at the launching hole (R_6)
	Damage to auxiliary facilities (R_7)
	Equipment damage and object strike (R_8)
	Shield machine assembly error (R_9)
R_L	Insufficient reinforcement at the receiving hole (R_{10})
	Launching port seal failure (R_{11})
	Off axis at shield launching (R_{12})
	Unstable reaction frame (R_{13})
	Unqualified base at the launching hole (R_{14})
R_N	Undiscovered karst caves and obstacles (R_{15})
	Improper control of shield tunnelling line (R_{16})
	Unsteady working face and water gushing (R_{17})
	Jack failure (R_{18})
	Shield posture out of control (R_{19})
	Shield tail seal failure (R_{20})
	Pressure loss of slurry sump (R_{21})
	Operation with pressure in warehouse (R_{22})
	Unqualified mud (R_{23})
	Improper grouting technology and parameters (R_{24})
	Unqualified tunnel segment (R_{25})
	Improper segment assembly (R_{26})
	Settlement of adjacent structures (R_{27})
R_R	Off axis at shield receiving (R_{28})
	Insufficient reinforcement at the receiving hole (R_{29})
	Receiving port seal failure (R_{30})
	Unqualified base at the receiving hole (R_{31})
	Instability at the shield receiving hole (R_{32})
	Shield machine disassembly error (R_{33})

conduction network shown is a directed graph, which contains 5 nodes and 10 directed edges. The directed edges represent the conduction path of the risk flow from the forward node to the backward node.

3.1.3. Causality Test of Risk Conduction Network. Based on the abovementioned risk conduction network, the structural equation model (SEM) is used for confirmatory factor analysis to test the causal relationship (conduction relationship) between various risk factors. There are exogenous observed variables, endogenous observed variables, exogenous latent variables, and endogenous latent variables in the SEM. In terms of model structure, SEM is divided into two parts: measurement equation and structural equation [27].

The measurement equation is used to describe the relationship between the observed variable and the latent variable, and the expression is as follows:

$$\begin{aligned} x &= \Lambda_x \xi + \delta, \\ y &= \Lambda_y \eta + \varepsilon. \end{aligned} \tag{1}$$

Here, x is the vector composed of exogenous observation variables; y is the vector composed of endogenous observation variables; Λ_x is the factor loading matrix of the exogenous observed variable on the exogenous latent variable. Λ_y is the factor loading of the endogenous observed variable on the endogenous latent variable; δ is the error term of the exogenous observation variable; and ε is the error term of the endogenous observation variable.

The structural equation is used to describe the relationship between latent variables, and the expression is as follows:

$$\eta = B\eta + \gamma\xi + \zeta. \tag{2}$$

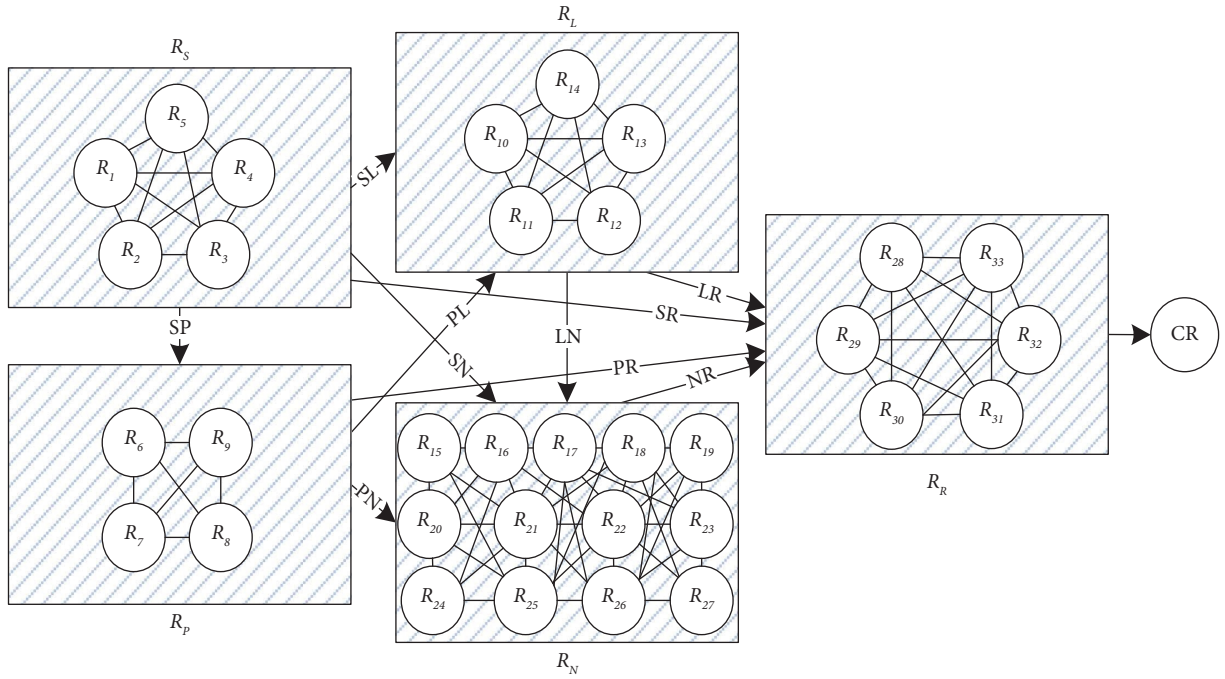

Figure 3: Risk conduction network.

Here, η is the endogenous latent variable; ξ is an exogenous latent variable; B is the relation between endogenous potential variables; γ is the influence of exogenous latent variables on endogenous latent variables; and ζ is the residual term of the structural equation, reflecting the unexplained part of η in the equation.

SEM can process multiple correlated and complex independent variables at the same time and has a powerful deautocorrelation function. Therefore, the risk factors in Figure 3 can be set as the observed variables of the SEM, each node is set as a latent variable, and the measurement equation between the observed variable and the latent variable is established according to the subordination relationship.

According to the previous description, the SEM of risk causality is established, as shown in Figure 4. There are 5 latent variables (R_S, R_P, R_L, R_N, and R_R) and 33 observed variables (R_1, R_2, . . ., R_{33}) in the model. e_1, e_2, . . ., e_{33} are the error terms of the observation variables; e_S, e_P, e_L, e_N, and e_R are the error terms of the latent variables; λ_1, λ_2, . . ., λ_{33} are the path coefficients corresponding to the 33 observation variables.

The questionnaire was designed using the Likert scale. Questionnaires completed by 173 people who had participated in underwater or shield tunnels were accepted. It is suggested in reference [28] that the sample size is greater than 10 times of the number of indicators (latent variables) and 5 times of the number of free parameters (observed variables), and the sample size of 173 meets that. After preprocessing, the data were processed by Cronbach'sα reliability test. SEM modeling software AMOS is used for the analysis [29]. The path map was made in the drawing interface, and the questionnaire data were read. After running the software with click "calculate estimates," the nonstandardized estimates of each path coefficient are obtained and transformed into standardized estimates. The calculation results are provided in Table 2.

3.2. Risk Conduction Mechanism Based on Fragility

3.2.1. Fragility Research. The premise of analyzing the risk conduction mechanism based on fragility is to identify the fragility factors of submarine tunnel shield construction. Based on the literature methodology and on-the-spot interview, 27 potential factors affecting the fragility of submarine tunnel shield construction are extracted. Referring to the subsystem classification of project management theory, the fragility factors of submarine tunnel shield construction are divided into 4 dimensions (F_i, $i = 1, 2, 3, 4$): target system fragility (F_1), object system fragility (F_2), organization system fragility (F_3), and behavior system fragility (F_4) [30]. Moreover, each dimension corresponds to different fragility factors ($F_{i.j}$), as shown in Table 3.

In order to investigate the importance of each fragility factor in its fragility dimension and the different performance of each dimension of fragility under the risk flow at different stages, the fragility of submarine tunnel shield construction is investigated by interview. The fragility dimensions and fragility factors are set as variables, respectively, and numbered as F_i and $F_{i.j}$.

Table 4 shows the weights ($\omega_{i.j}$) of fragility factors in their fragility dimensions.

Fragility is specific to the risk flow at a specific stage. In the face of risk flow at different stages, each dimension of fragility shows different states, which are defined as F_x ($x = S$, P, L, N, and R). Therefore, the contribution (μ_{x-i}) of each

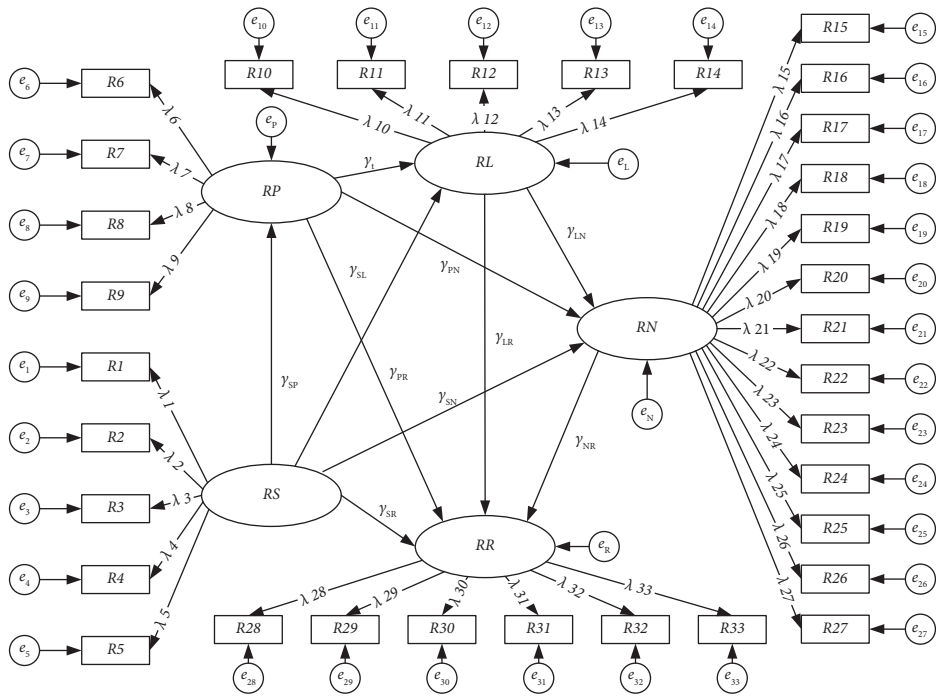

Figure 4: SEM of risk causality.

Table 2: Path coefficient.

R_X	R_i	Nonstandardized estimates	Standardized estimates
R_S	R_1	0.735	0.246
	R_2	0.474	0.159
	R_3	0.653	0.219
	R_4	0.425	0.142
	R_5	0.698	0.234
R_P	R_6	0.667	0.259
	R_7	0.859	0.333
	R_8	0.485	0.188
	R_9	0.568	0.220
R_L	R_{10}	0.635	0.174
	R_{11}	0.762	0.209
	R_{12}	0.498	0.137
	R_{13}	0.856	0.235
	R_{14}	0.897	0.246
R_N	R_{15}	0.896	0.101
	R_{16}	0.578	0.065
	R_{17}	0.486	0.055
	R_{18}	0.589	0.066
	R_{19}	0.832	0.093
	R_{20}	0.689	0.077
	R_{21}	0.798	0.090
	R_{22}	0.687	0.077
	R_{23}	0.635	0.071
	R_{24}	0.632	0.071
	R_{25}	0.487	0.055
	R_{26}	0.739	0.083
	R_{27}	0.861	0.097
R_R	R_{28}	0.453	0.118
	R_{29}	0.419	0.109
	R_{30}	0.634	0.165
	R_{31}	0.726	0.189
	R_{32}	0.881	0.229
	R_{33}	0.728	0.190

Table 3: Fragility factors.

F_i	$F_{i.j}$
F_1	Project importance ($F_{1.1}$)
	Political and economic stability ($F_{1.2}$)
	Public support ($F_{1.3}$)
	Market demand ($F_{1.4}$)
	Ecological environmental conditions ($F_{1.5}$)
	Standardization of bidding ($F_{1.6}$)
F_2	Construction scale ($F_{2.1}$)
	Total investment ($F_{2.2}$)
	Geographical location ($F_{2.3}$)
	Project complexity ($F_{2.4}$)
F_3	Contract completeness ($F_{3.1}$)
	Organizational structure rationality ($F_{3.2}$)
	Participant partnership ($F_{3.3}$)
	Government support ($F_{3.4}$)
	Complexity of the approval process ($F_{3.5}$)
	Design and construction unit qualification ($F_{3.6}$)
	Rationality of selection of suppliers ($F_{3.7}$)
F_4	Financing efficiency ($F_{4.1}$)
	Geological prospecting accuracy ($F_{4.2}$)
	Rationality of design plan ($F_{4.3}$)
	Contractor project management capabilities ($F_{4.4}$)
	Proprietor project management capabilities ($F_{4.5}$)
	Tool management capability ($F_{4.6}$)
	Advanced geological prediction accuracy ($F_{4.7}$)
	Emergency plan rationality ($F_{4.8}$)
	Communication and coordination ability ($F_{4.9}$)
	Safety education ($F_{4.10}$)

Table 4: The weights of fragility factors in their dimensions.

F_i	$F_{i.j}$	Mean	Variance	$\omega_{i.j}$
F_1	$F_{1.1}$	3.630	0.302	0.168
	$F_{1.2}$	3.549	0.340	0.164
	$F_{1.3}$	3.566	0.361	0.165
	$F_{1.4}$	3.590	0.265	0.166
	$F_{1.5}$	3.561	0.316	0.165
	$F_{1.6}$	3.711	0.414	0.172
F_2	$F_{2.1}$	3.688	0.400	0.250
	$F_{2.2}$	3.543	0.456	0.240
	$F_{2.3}$	3.792	0.396	0.257
	$F_{2.4}$	3.717	0.330	0.252
F_3	$F_{3.1}$	3.671	0.371	0.144
	$F_{3.2}$	3.572	0.256	0.140
	$F_{3.3}$	3.584	0.347	0.141
	$F_{3.4}$	3.705	0.416	0.145
	$F_{3.5}$	3.624	0.385	0.142
	$F_{3.6}$	3.746	0.247	0.147
	$F_{3.7}$	3.584	0.382	0.141
F_4	$F_{4.1}$	3.590	0.427	0.096
	$F_{4.2}$	3.873	0.261	0.104
	$F_{4.3}$	3.497	0.377	0.094
	$F_{4.4}$	3.572	0.360	0.096
	$F_{4.5}$	3.636	0.370	0.098
	$F_{4.6}$	3.451	0.363	0.093
	$F_{4.7}$	3.925	0.405	0.105
	$F_{4.8}$	3.879	0.407	0.104
	$F_{4.9}$	3.873	0.516	0.104
	$F_{4.10}$	3.954	0.426	0.106

dimension of fragility should depend on the risk flow at a specific stage. The contributions of the dimension of fragility are shown in Table 5.

3.2.2. Risk-Fragility Process Analysis. The development direction of the risk in the system is closely related to the fragility, and risk and fragility together constitute the risk-fragility (R-F) process. In the risk conduction process, the risk event is equivalent to the risk issuer. When the accumulation of risk energy reaches a critical level, it appears as a sudden risk event. The risk result is relative to the risk event. The risk result is often used to replace the risk receiver, which refers to the consequences caused by the risk event. Risk is conducted in the form of energy, and the energy at the network node is expressed as a risk state contained in the system. In the R-F process, the risk result is the result of the joint effect of the risk event and the fragility. The fragility is equivalent to the role of the risk conduction carrier and the risk conduction, and the value of the fragility reflects the resistance of the risk conduction carrier. It has also become a path for the intrusion of risk events. Figure 5 shows the fragility (F_{xy}) of each risk conduction process in the risk conduction network.

The submarine tunnel shield construction has experienced 4 discrete time nodes t_p, t_l, t_n, and t_r, corresponding to the time midpoints of each stage T_p, T_l, T_n, and T_r. When each stage (S, P, L, N, and R) is attacked by risks, the system shows different fragility, namely, $F_S(t)$, $F_P(t)$, $F_L(t)$, $F_N(t)$, and $F_R(t)$, and its state changes with time.

It can be seen from the above that in the risk conduction network, there are three key risk variables: risk event (R), risk result (Result$R$), and risk state (State$R$).

Risk result refers to the consequence of the risk event. The submarine tunnel shield construction system is approximately described as a linear time-varying system, so there is a linear relationship between the risk result Result$R_{ij}(s)$ and the risk event $R_{ij}(s)$ in the R-F process, and the transmission function $W(s)$ can be used to represent the process of transmitting the risk event to the risk result. Formula (4) is determined by [31].

$$\text{Result}R_{ij}(s) = R_{ij}(s)W(s), \tag{3}$$

$$W(s) = 1 - e^{-\theta \int_0^s e^{F(t)} \mathrm{d}t}. \tag{4}$$

Here, s represents the time range of the risk event action and θ represents the baseline risk rate. $F(t)$ is the fragility of the risk construction path.

The risk state of each node is determined by its own risk energy and the risk energy conducted from the forward edge of the node. That is, the risk state StateR_j of each stage is jointly determined by the risk result produced by the node Result$R_{jj}(s)$ and the risk result conducted from the forward edge of the node Result$R_{ij}(s)$. It is manifested by the coupling between the risk results on different construction paths at the same stage. The coupling formula (5) is determined by [32].

Table 5: The contributions of the dimension of fragility.

F_x	F_i	Mean	Variance	μ_{x-i}
F_S	F_1	3.873	0.261	0.263
	F_2	3.572	0.256	0.242
	F_3	3.711	0.414	0.252
	F_4	3.590	0.265	0.243
F_P	F_1	3.630	0.302	0.251
	F_2	3.549	0.340	0.245
	F_3	3.717	0.330	0.257
	F_4	3.590	0.427	0.248
F_L	F_1	3.705	0.416	0.256
	F_2	3.624	0.385	0.250
	F_3	3.566	0.361	0.246
	F_4	3.584	0.347	0.248
F_N	F_1	3.688	0.400	0.255
	F_2	3.671	0.371	0.254
	F_3	3.543	0.456	0.245
	F_4	3.561	0.316	0.246
F_R	F_1	3.584	0.382	0.245
	F_2	3.497	0.377	0.239
	F_3	3.792	0.396	0.259
	F_4	3.746	0.247	0.256

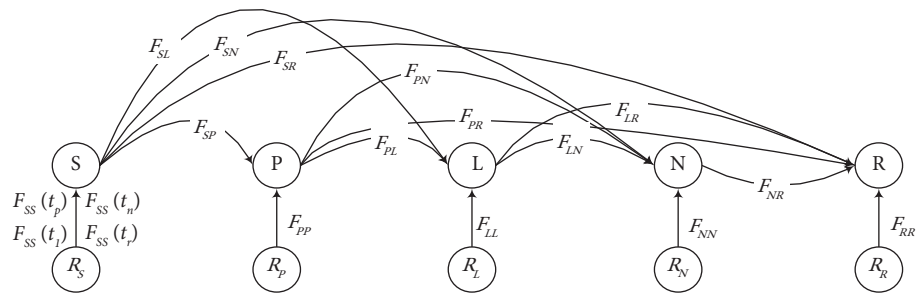

Figure 5: Fragility in the risk conduction process.

$$\text{State}R_j(s) = \sum_{i=s,p,\ldots,j}^{j} \text{Result}R_{ij}(s) + 2 \sum_{\substack{m=s,p,\ldots,j \\ n=\text{m}+1,\ldots,j}} \rho_{mn} \sqrt{\text{Result}R_{mj}(s)} \sqrt{\text{Result}R_{nj}(s)}. \tag{5}$$

Here, ρ_{mn} represents the correlation coefficient between risk result i and risk result j, which can be considered as the coupling degree between them. $|\rho_{mn}| \le 1$.

The risk event $R_{ij}(s)$ of node j is obtained from the risk flow occurring at node j. In addition, the diffusion effect of the risk state $\text{State}R_i(s)$ that occurred at the previous node i is also considered. That is, the risk event $R_{ij}(s)$ is determined by the diffusion function $D_{ij}(s)$ from node i to node j and the risk state $\text{State}R_i(s)$ of node i. The risk state is prioritized to diffuse to the risk conduction path with weak antirisk ability [33]. Therefore, the diffusion function can be determined according to the fragility as follows:

$$R_{ij}(s) = \text{State}R_i(s) D_{ij}(s), \tag{6}$$

$$D_{ij}(s) = \Omega_{ij} = \frac{\int_0^s F_{ij}(t)\text{d}t}{\sum_{j=1}^{n} \int_0^s F_{ij}(t)\text{d}t}. \tag{7}$$

Here, s represents the time range of the risk state action. $F_{ij}(t)$ is the fragility of the risk conduction path.

3.2.3. Dynamic Fragility Assessment. As can be seen from the abovementioned R-F process, the dynamic fragility assessment is a prerequisite for the realization of CR control. Here are the steps of dynamic fragility assessment.

Step 1. The initial value of fragility factors of a specific project is evaluated by referring to expert opinions or similar project experience. The control measures to decrease fragility are collected and sorted out. The fragility factors and construction stages that the control measures act on need to be judged, and the dynamic value of fragility factors $F_{i,j}(t)$ can be calculated.

Step 2. Based on $F_{i,j}(t)$, the dynamic value of the fragility dimension $F_i(t)$ is evaluated according to formula (8).

$$F_i(t) = \sum_{j=1}^{k} \omega_{ij} F_{i.j}(t). \tag{8}$$

Here, $i = 1, 2, 3, 4$. $j = 1, 2, \ldots, k$. k is the number of fragility factors corresponding to the fragility dimension; ω_{ij} is the weight corresponding to $F_{i,j}(t)$, which can be found in Table 4.

Step 3. Based on $F_i(t)$, the fragility state value $F_x(t)$ under the risk flow at a specific stage can be evaluated according to formula (9).

$$F_x(t) = \sum_{i=1}^{4} \mu_{x-j} F_i(t). \tag{9}$$

Here, $x = S, P, L, N, R$. μ_{x-j} is the weight corresponding to $F_i(t)$, which can be found in Table 5.

Step 4. Based on $F_x(t)$, the fragility of the risk conduction process F_{xy} is evaluated. The calculation process is performed according to Tables 6 and 7. Table 6 shows the formulas for regression coefficients β of F_{xy}, and Table 7 shows the formulas for solving F_{xy}.

3.3. CR Control Model for Submarine Tunnel Shield Construction. Relative to the uncertainty of risk, fragility is an internal attribute of the system. Appropriate control measures can be taken to reduce the fragility of the risk conduction network so that the risk results will develop in a favorable direction and ensure that the risk state of the system is at a low level to realize control of CR. Based on the introduction of the causal loop diagram in Section 2.3, the risk conduction network in Section 3.1, and the R-F process in Section 3.2, the causal loop diagram of CR control for submarine tunnel shield construction, as shown in Figure 6, is constructed to facilitate the description of the causal relationship between the variables of the model.

It can be seen from Figure 6 that the risk conduction network is complex, the control process covers a large amount of information, and the time node span is long. It was difficult to be realized by human calculation. Therefore, it is necessary to use the simulation software VENSIM special for SD to model and simulate the CR control system for submarine tunnel shield construction. As the model is complex, the SD model is divided into two modules, which are the feedback control module and the risk conduction network module.

The feedback control module is mainly based on the dynamic feedback mechanism. The CR feedback from the system is converted into a signal that acts on the fragility of the risk conduction network. Its purpose is to use the system state at the previous moment to influence the risk conduction at the next moment so as to realize the control of CR. The SD flow diagram of the feedback control module is shown in Figure 7.

The risk conduction network module mainly simulates the whole process of the risk conduction. In order to understand this module intuitively and clearly, it is decomposed and laid out according to the submarine tunnel shield construction stages, as shown in Figure 8.

4. Empirical Research

Dalian Metro Line 5 Cross-sea Large Diameter Shield Construction Project has a total length of 3310 m, of which the submarine shield tunnel section is 2310 m. The 12.26 m diameter slurry balanced large shield was used for construction. Faced with the four major problems of traversing areas with strong karst development, large-diameter and long-distance hard rock excavation, high-water pressure large shield sealing and silo operation under pressure, and tunnelling under important structures, the construction is very difficult. There is no precedent for the project at home and abroad, and it is classified as a "global problem" by industry experts. In this paper, Dalian Metro Line 5 Cross-sea Large Diameter Shield Construction Project (case project for short) is selected as an empirical study. The schematic diagram of the tunnel line of the shield is shown in Figure 9. The total project duration is 43 months, including 13 months in the preparing stage, 4 months in the launching stage, 20 months in the normal tunnelling stage, and 6 months in the receiving stage.

4.1. Data Acquisition

4.1.1. Risk Factors. The risk is divided into five levels from 1 to 5: slight risk, general risk, significant risk, high risk, and extremely high risk by the LEC risk evaluation method, and the unit is set to level. After studying and judging the information of the case project and consulting the opinions of experts, the initial value of the risk factors of the case project was obtained. The initial value of the risk flow at different stages is solved through the path coefficient in Section 3.1.3. The calculation results are shown in Table 8.

4.1.2. Fragility and Control Measure. Through field observation and document analysis of case projects, combined with the opinions of builders and experts, the initial value of each fragility factor $F_{i,j}(t_p)$ is obtained. As shown in Table 9, the fragility factors are divided into five levels from 1 to 5. The higher the value is, the higher the fragility is, and the unit is set to level. A variety of control measures were taken to reduce the fragility during the construction of the case project, and they are summarized in Table 10 ($X\ F_{i,j}$) means that the control measures (M_i, $i = 1, 2, \ldots, 11$) act on the

Table 6: The contributions of the dimension of fragility.

F_{xy}	s_p	s_l	s_n	s_r	β_p	β_l	β_n	β_r
F_{SS}					1	1	1	1
F_{SP}					1	0	0	0
F_{SL}					0	1	0	0
F_{SN}					0	0	1	0
F_{SR}					0	0	0	1
F_{PP}					1	0	0	0
F_{PL}	T_p /2	T_l /2			$s_p/(s_p+s_l)$	$s_l/(s_p+s_l)$	0	0
F_{PN}	T_p /2	T_l	T_n /2		$s_p/(s_p+s_l+s_n)$	$s_l/(s_p+s_l+s_n)$	$s_n/(s_p+s_l+s_n)$	0
F_{PR}	T_p /2	T_l /2	T_n	T_r /2	$s_p/(s_p+s_l+s_n+s_r)$	$s_l/(s_p+s_l+s_n+s_r)$	$s_n/(s_p+s_l+s_n+s_r)$	$s_r/(s_p+s_l+s_n+s_r)$
F_{LL}					0	1	0	0
F_{LN}		T_l	T_n /2		0	$s_l/(s_l+s_n)$	$s_n/(s_l+s_n)$	0
F_{LR}		T_l /2	T_n	T_r /2	0	$s_l/(s_l+s_n+s_r)$	$s_n/(s_l+s_n+s_r)$	$s_r/(s_l+s_n+s_r)$
F_{NN}					0	0	1	0
F_{NR}			T_n /2	T_r /2	0	0	$s_n/(s_n+s_r)$	$s_r/(s_n+s_r)$

Table 7: The calculation formulas of F_{xy}.

F_{xy}	t_p	t_l	t_n	t_r	F_{xy}
F_{SS}	$F_S(t_p)$	$F_S(t_l)$	$F_S(t_n)$	$F_S(t_r)$	$F_{SS}=\beta_pF_S(t_p)\vee\beta_lF_S(t_l)\vee\beta_nF_S(t_n)\vee\beta_rF_S(t_r)$
F_{SP}	$F_P(t_p)$				$F_{SP}=\beta_pF_P(t_p)$
F_{SL}		$F_L(t_l)$			$F_{SL}=\beta_lF_L(t_l)$
F_{SN}			$F_N(t_n)$		$F_{SN}=\beta_nF_N(t_n)$
F_{SR}				$F_R(t_r)$	$F_{SR}=\beta_rF_R(t_r)$
F_{PP}	$F_P(t_p)$				$F_{PP}=\beta_pF_P(t_p)$
F_{PL}	$F_L(t_p)$	$F_L(t_l)$			$F_{PL}=\beta_pF_L(t_p)+\beta_lF_L(t_l)$
F_{PN}	$F_N(t_p)$	$F_N(t_p)$	$F_N(t_p)$		$F_{PN}=\beta_pF_N(t_p)+\beta_lF_N(t_p)+\beta_nF_N(t_p)$
F_{PR}	$F_R(t_p)$	$F_R(t_l)$	$F_R(t_n)$	$F_R(t_r)$	$F_{PR}=\beta_pF_R(t_p)+\beta_lF_R(t_l)+\beta_nF_R(t_n)+\beta_rF_R(t_r)$
F_{LL}		$F_L(t_l)$			$F_{LL}=\beta_lF_L(t_l)$
F_{LN}		$F_N(t_l)$	$F_N(t_n)$		$F_{LN}=\beta_lF_N(t_l)+\beta_nF_N(t_n)$
F_{LR}		$F_R(t_l)$	$F_R(t_n)$	$F_R(t_r)$	$F_{LR}=\beta_lF_R(t_l)+\beta_nF_R(t_n)+\beta_rF_R(t_r)$
F_{NN}			$F_N(t_n)$		$F_{NN}=\beta_nF_N(t_n)$
F_{NR}			$F_R(t_n)$	$F_R(t_r)$	$F_{NR}=\beta_nF_R(t_n)+\beta_rF_R(t_r)$

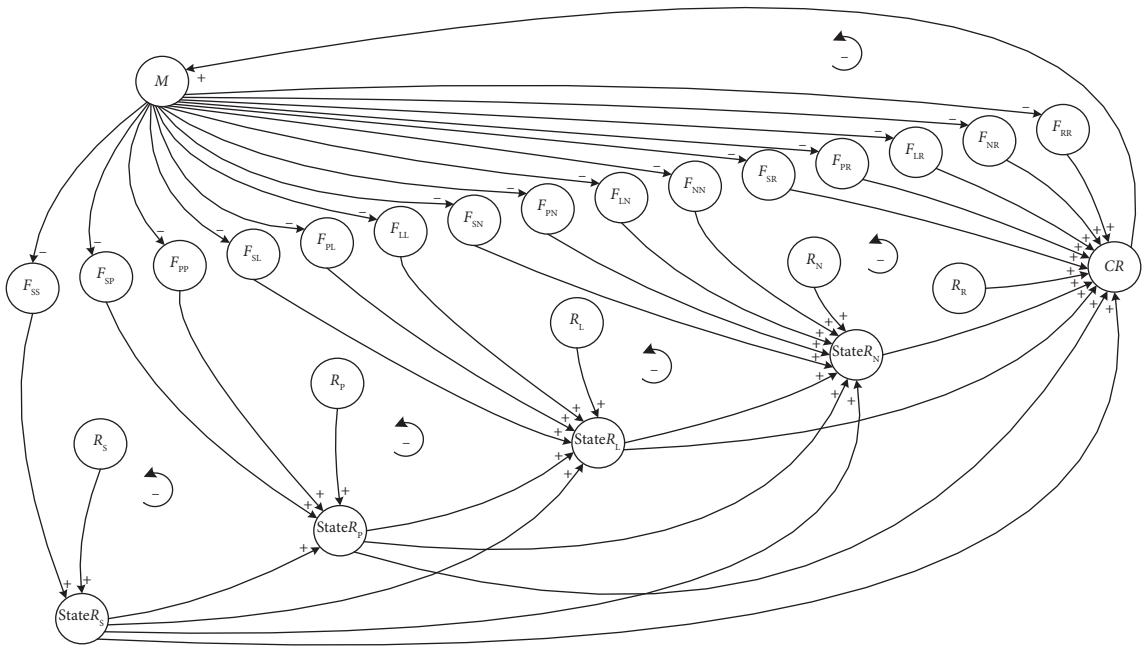

Figure 6: Causal loop diagram of CR control for submarine tunnel shield construction.

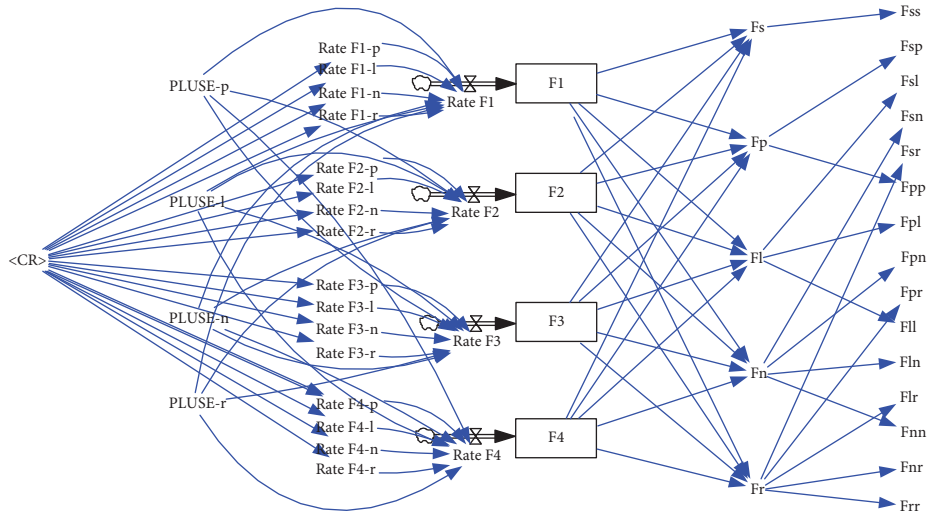

Figure 7: The SD flow diagram of the feedback control module.

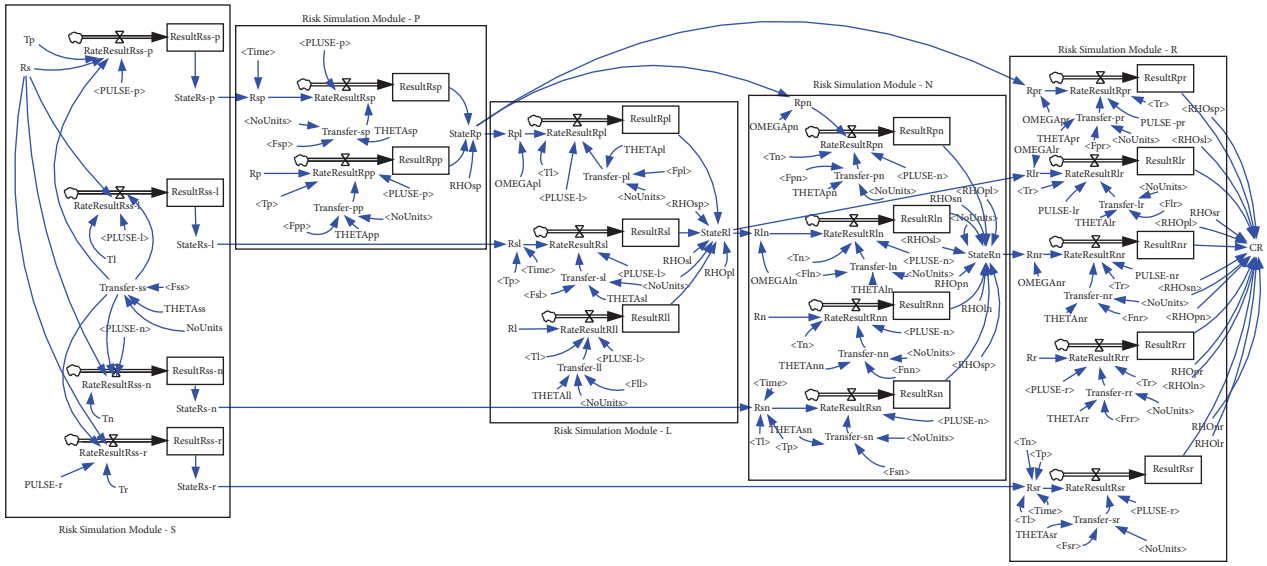

Figure 8: The SD flow diagram of the risk conduction network module.

fragility factor $F_{i.j}$ during the construction stage X. Assuming that the effects of various control measures are consistent, the amount of change to the fragility factor is −1. The change of fragility in each stage is shown in the dynamic value of fragility factor $F_{i.j}(t)$ in Table 9.

Based on $F_{i.j}(t)$, the dynamic value of fragility dimension $F_i(t)$ is calculated according to formula (8), and the calculation results are shown in Table 9. Then, the system fragility state value under the risk flow at a specific stage $F_x(t)$ is calculated according to formula (9), and the calculation results are shown in Table 11.

Based on $F_x(t)$, the fragility F_{xy} of the risk conduction process can be calculated according to the calculation process in Tables 6 and 7. Here, $t_p = 4$, $t_l = 20$, $t_n = 6$, and $t_r = 13$, and the calculation results are shown in Table 12.

4.2. Model Initialization. Through the calculation mentioned, all kinds of data needed to be input for SD model simulation are obtained. Due to the writing limitation of the software, the variables in the actual model change in software VENSIM.

The name of the level variable F_i in the software is F_i, its initial value is the data in the $F_i(t_p)$ column in Table 9, and the unit is level; the name of the ResultR_{ij} in the software is ResultR_{ij}. At the beginning of the project, the risk has not yet occurred, so the initial value of the each risk result is 0, and the unit is level.

The name of the constant variable R_i in the software is R_i, its value is the data in Table 8, and the unit is level; the name of the t_i in the software is T_i, its value is the duration of each stage of the case project, and the unit is month; the single

Figure 9: The schematic diagram of the tunnel line of the shield.

Table 8: The initial value of risk factors and risk flows.

R_i	R_X	R_i	R_X
R_1	4		
R_2	1		
R_3	4	R_S	3.096
R_4	1		
R_5	4		
R_6	3		
R_7	3	R_P	2.592
R_8	2		
R_9	2		
R_{10}	3		
R_{11}	3		
R_{12}	2	R_L	3.109
R_{13}	3		
R_{14}	4		
R_{15}	4		
R_{16}	3		
R_{17}	3		
R_{18}	3		
R_{19}	3		
R_{20}	3		
R_{21}	4	R_N	3.007
R_{22}	3		
R_{23}	2		
R_{24}	2		
R_{25}	2		
R_{26}	2		
R_{27}	4		
R_{28}	2		
R_{29}	2		
R_{30}	2	R_R	2.190
R_{31}	2		
R_{32}	2		
R_{33}	3		

pulse function PLUSE is also set based on the time distribution of each stage.

In addition, some coefficients are set as constants in the software, which are listed in Table 13. The coefficient θ_{ij} in formula (4) is named THETA*ij* in the software, which is 0.2 according to the literature [34]. The coefficient Ω_{ij} in formula (7) is named OMEGAij in the software, and its value is calculated according to the formula. The coefficient ρ_{ij} in formula (5) is named RHOij in the software, and its value is obtained by the Delphi method.

Before the simulation, the model needs to be set. The INITIAL TIME is 0, the FINAL TIME is 43, the TIME STEP is 1, the units for time is month, and it is set to 'Save results every TIME STEP."

The structural dimension test, stability test, and extreme condition test are used to investigate the logic, stability, and reliability of the model. The structural dimension test can be completed directly through the functions of "Check Model" and "Units Check" in the software VENSIM, and the results show that the model meets the test requirements. In the stability test, changes in model simulation results under different time steps (0.125 month, 0.25 month, and 1 month) were investigated. As shown in Figure 10, CR with different time steps has the same development trend and little difference, indicating that the model has good stability. In the extreme condition test, the initial value of risk factors and fragility factors are taken as key factors to investigate the simulation situation of the model when the key factors are in an extreme state. Figure 11(a) shows the model simulation results when the initial value of risk factors are 0 and 5, respectively. When the value is 0, it means that the risk does not exist, CR always takes a value of 0 during the simulation cycle, and when it takes a value of 5, CR shows an upward trend, and it tends to be flat under the influence of fragility in

Table 9: The dynamic value of $F_{i.j}$ (t) and F_i (t).

$F_{i.j}$	$F_{i.j}$ (t)					F_i (t)				
	$\omega_{i.j}$	$F_{i.j}$ (t_p)	$F_{i.j}$ (t_l)	$F_{i.j}$ (t_n)	$F_{i.j}$ (t_R)	F_i (t)	F_i (t_p)	F_i (t_l)	F_i (t_n)	F_i (t_R)
$F_{1.1}$	0.168	2	2	2	2					
$F_{1.2}$	0.164	2	2	2	2					
$F_{1.3}$	0.165	2	1	1	1	F_1	2.000	1.670	1.670	1.670
$F_{1.4}$	0.166	2	2	2	2					
$F_{1.5}$	0.165	2	1	1	1					
$F_{1.6}$	0.172	2	2	2	2					
$F_{2.1}$	0.250	3	2	2	2					
$F_{2.2}$	0.240	4	3	3	2	F_2	3.750	2.498	1.993	1.753
$F_{2.3}$	0.257	4	3	3	3					
$F_{2.4}$	0.252	4	2	0	0					
$F_{3.1}$	0.144	3	3	3	3					
$F_{3.2}$	0.140	2	2	2	2					
$F_{3.3}$	0.141	2	2	2	2					
$F_{3.4}$	0.145	4	4	4	2	F_3	2.719	2.577	2.577	2.286
$F_{3.5}$	0.142	4	3	3	3					
$F_{3.6}$	0.147	2	2	2	2					
$F_{3.7}$	0.141	2	2	2	2					
$F_{4.1}$	0.096	2	2	2	2					
$F_{4.2}$	0.104	4	3	2	2					
$F_{4.3}$	0.094	3	2	2	2					
$F_{4.4}$	0.096	2	2	0	0					
$F_{4.5}$	0.098	2	2	0	0	F_4	2.905	2.601	1.726	1.414
$F_{4.6}$	0.093	4	4	1	1					
$F_{4.7}$	0.105	3	3	2	2					
$F_{4.8}$	0.104	3	3	3	2					
$F_{4.9}$	0.104	4	4	4	2					
$F_{4.10}$	0.106	2	1	1	1					

Table 10: The control measures and effects.

M_i	Control measures	Effects
M_1	Single-hole double-track tunnel design plan	(P $F_{1.3}$, $F_{1.5}$, $F_{2.1}$, $F_{2.2}$, $F_{2.4}$, $F_{3.5}$, $F_{4.2}$, $F_{4.3}$); (L $F_{4.6}$)
M_2	Geological treatment before excavation	(P $F_{2.3}$, $F_{2.4}$)
M_3	Air-cushion pressure-regulating mud-water balance shield machine equipped with large-flow mud-water scouring cycle and secondary crusher	(L $F_{2.4}$)
M_4	Replacement of the disc cutters under atmospheric conditions, telescopic spherical hinge main drive	(L $F_{2.4}$, $F_{4.6}$)
M_5	Advance drill, advance grouting system, and advanced geophysical equipment	(L $F_{2.4}$, $F_{4.2}$, $F_{4.7}$)
M_6	Improved wear resistance of disc cutters	(L $F_{2.4}$, $F_{4.6}$)
M_7	Construction of structural health monitoring and intelligent safety early warning system	(L $F_{4.4}$, $F_{4.5}$)
M_8	Closed construction during COVID-19	(N $F_{2.2}$, $F_{3.4}$)
M_9	Real-time remote monitoring system	(L $F_{4.4}$, $F_{4.5}$); (N $F_{4.9}$)
M_{10}	Tunnel communication extension system	(N $F_{4.4}$, $F_{4.9}$)
M_{11}	Emergency drill for various accidents	(N $F_{3.4}$, $F_{4.4}$, $F_{4.8}$); (P $F_{4.10}$)

the later period, which is in line with the actual situation. Figure 11(b) shows the model simulation results when the initial values of fragility factors are 0 and 5, respectively. When the values are 0, the system has an ideal high risk resistance ability, and the risk cannot be conducted, and CR always takes a value of 0 within the simulation cycle. When the value is 5, the system does not have the ability to resist risks; CR shows a malignant growth trend and reaches the level of extremely high risk in a short time, which is consistent with the actual situation. The abovementioned statement shows that the model has good reliability.

4.3. Results and Discussion. After completing the settings of variables, constant variables, and auxiliary variables, the model is revised and passed the Check Model and Units Check. The model is allowed to simulate, and the simulation results of CR are obtained, as shown by the blue line in Figure 12.

The conclusion can be drawn from the figure: ① CR showed an upward trend with the passage of time, indicating that risks continue to accumulate in the risk conduction network, forming a cumulative effect. ② In the later period, the rising curve of CR gradually flattened, indicating that

Table 11: The dynamic value of $F_x(t)$.

Fx	μ_{x-i}		$F_x(t_p)$	$F_x(t_l)$	$F_x(t_n)$	$F_x(t_R)$
F_S	F_1	0.263	2.825	2.325	1.990	1.783
	F_2	0.242				
	F_3	0.252				
	F_4	0.243				
F_P	F_1	0.251	2.837	2.336	1.996	1.785
	F_2	0.245				
	F_3	0.257				
	F_4	0.248				
F_L	F_1	0.256	2.839	2.331	1.988	1.779
	F_2	0.250				
	F_3	0.246				
	F_4	0.248				
F_N	F_1	0.255	2.843	2.331	1.988	1.779
	F_2	0.254				
	F_3	0.245				
	F_4	0.246				
F_R	F_1	0.245	2.837	2.342	1.997	1.784
	F_2	0.239				
	F_3	0.259				
	F_4	0.256				

Table 12: The calculation formulas of F_{xy}.

F_{xy}	$F_{SS}(t_p)$	$F_{SS}(t_l)$	$F_{SS}(t_n)$	$F_{SS}(t_R)$	F_{SP}	F_{SL}	F_{SN}	F_{SR}	F_{PP}	F_{PL}	F_{PN}	F_{PR}	F_{LL}	F_{LN}	F_{LR}	F_{NN}	F_{NR}
	2.825	2.325	1.990	1.783	2.837	2.331	1.988	1.784	2.837	2.719	2.326	2.182	2.331	2.045	1.999	1.988	1.948

Table 13: The value of the coefficient.

Coefficient	Value
THETAsp	0.2
THETApp	0.2
THETApl	0.2
THETAsl	0.2
THETAll	0.2
THETApn	0.2
THETAln	0.2
THETAnn	0.2
THETAsn	0.2
THETApr	0.2
THETAlr	0.2
THETAnr	0.2
THETArr	0.2
RHOsp	0.650
RHOsl	−0.825
RHOpl	0.775
RHOsn	−0.600
RHOpn	−0.925
RHOln	−0.495
RHOsr	−0.950
RHOpr	−0.429
RHOnr	−0.775
RHOlr	0.875
OMEGApl	0.376
OMEGApn	0.322
OMEGApr	0.302
OMEGAln	0.506
OMEGAlr	0.494
OMEGAnr	1.000

under the control measures, the risk has been effectively controlled. ③ The maximum value of CR is within 3.00, a general risk. This shows that normal construction can be carried out, but risk management and control still need to be paid attention to. The red line in Figure 12 shows the trend of CR curve without control measures. The curve growth rate has accelerated significantly, and its value is 3.34 in the 22nd month, which indicates that the project has a significant risk at this time and should stop immediately; otherwise, with the progress of construction, the risk will continue to accumulate malignantly and will soon change to the high-risk state if the value exceeds 4.00, and finally, more than 5.00 will become a high-risk state in the 28th month, and at the end of the construction period, the 43rd month value will be 8.94.

In contrast, the CR value with the control measures only exceeded 2.00 (general risk) in the 36th month, which was effectively delayed for 18 months. In addition, the CR value at the end of the construction period (the 43rd month) is only 2.38, which is only 26.63% of that without control measures, and the control effect is significant. The simulation results conform to the objective facts of the case project, effectively illustrate the correctness of the model construction, and objectively reflect the changing laws of CR with the control measures.

The change curves of risk results and risk states are shown in Figure 13, which visually verifies the law of risk conduction: ① the risk state is conducted from the risk results of the forward edge of the node. In addition, it is formed by their coupling, not simple addition. For example, StateR_p, as shown in (a), is formed by the weak coupling

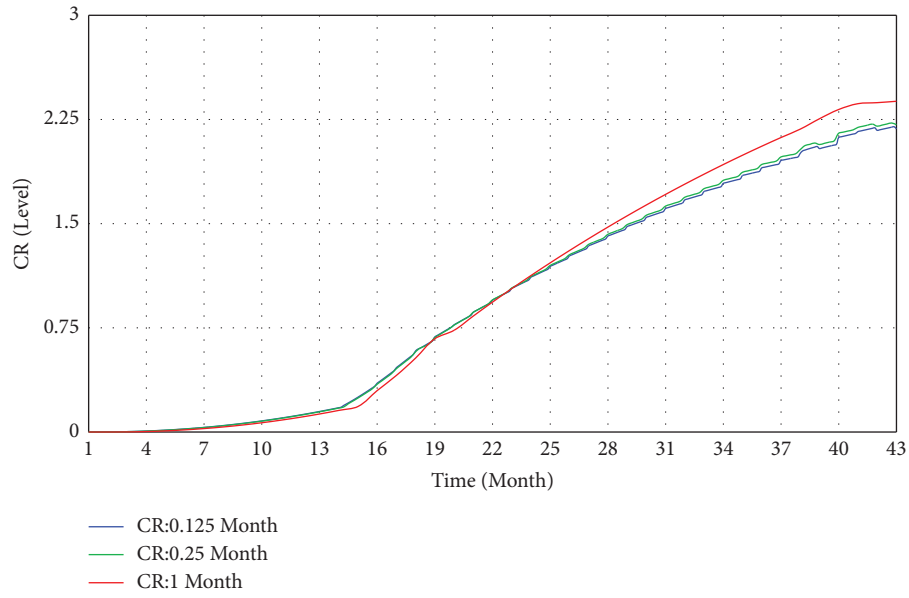

Figure 10: Stability test results.

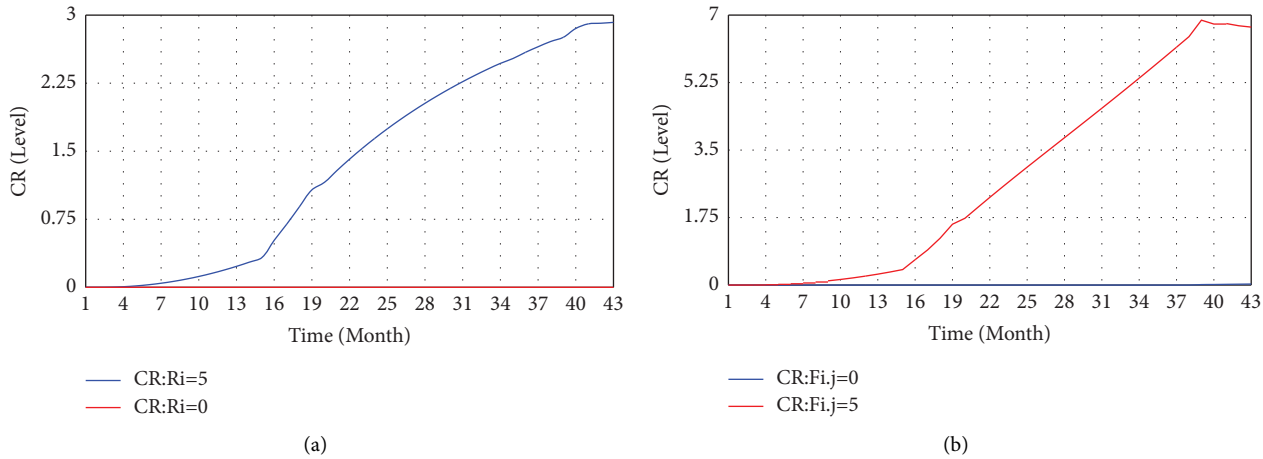

Figure 11: Extreme condition test results. (a) Risk factors. (b) Fragility factors.

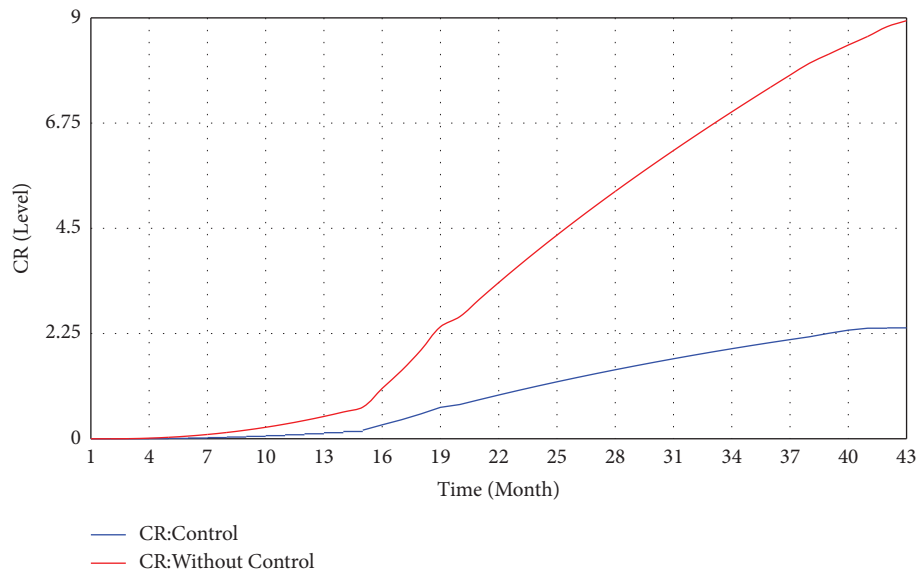

Figure 12: The simulation result of CR.

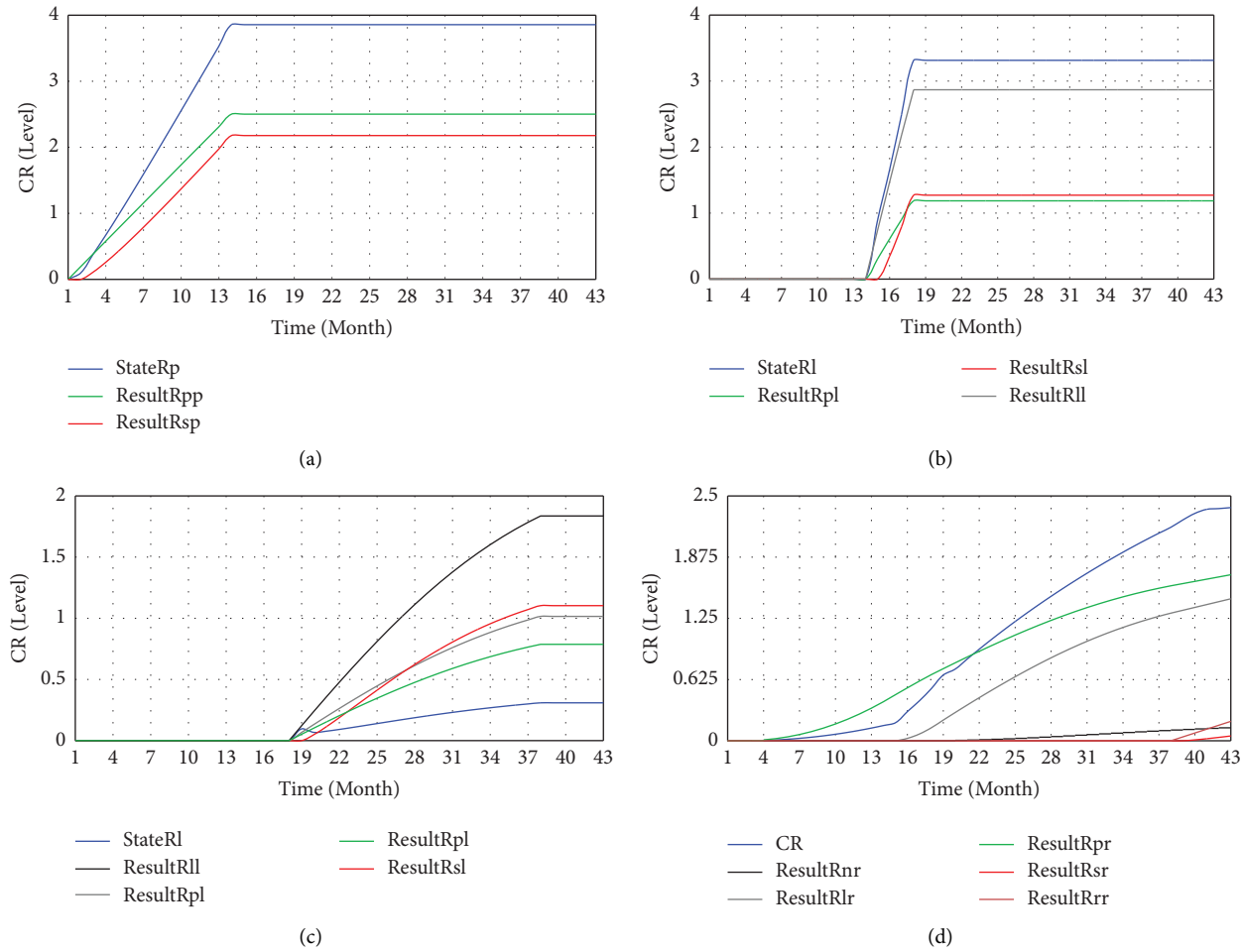

Figure 13: The simulation result of risk conduction network. (a) The simulation results of risk-preparation. (b) The simulation results of risk-launch. (c) The simulation results of risk-normal. (d) The simulation results of risk-receiving.

effect between $ResultR_{sp}$ and $ResultR_{pp}$. ② The risk state is transmitted to all backward nodes through the diffusion effect to form risk events. For example, R_{pl}, R_{pn}, and R_{pr} are distributed by $StateR_p$ according to the fragility weight of their respective risk conduction process. ③The control effect of each risk conduction process is reflected. For example, as shown in (d), due to the hysteresis effect of the control measures, the slowing trend of the preparing stage and the launching stage is not obvious, but the upward trend of the curve in the normal tunnelling stage and the receiving stage is obviously controlled.

5. Conclusions

(1) The introduction of CR is an important supplement to the existing risk management theory of submarine tunnel shield construction and the innovation of the risk management method of the engineering construction project.

(2) The risk factors of submarine tunnel shield construction are identified, and the risk conduction network is constructed with reference to the energy release theory. The confirmatory factor analysis is carried out by SEM to test the causal relationship between risk factors and determine the path coefficient of the risk conduction network.

(3) The transmission, diffusion, and coupling relationships among risk events, risk results, and risk states in risk conduction network are analyzed. The fragility factors of submarine tunnel shield construction are identified and evaluated, and the F_{xy} of the risk conduction process is obtained.

(4) SD is applied to construct the dynamic control model of cumulative risk of submarine tunnel shield construction, and the modeling simulation is carried out by taking Dalian Metro Line 5 Cross-sea Large Diameter Shield Construction Project as a case. The control measures acting on fragility can reduce the CR value at the end of construction from 8.94 (great risk) to 2.381 (general risk). Moreover, the state of general risk is delayed for 18 months. The simulation results conform to the objective facts of the case project, which verifies the correctness and effectiveness of the model, and can provide decision support for construction managers.

Data Availability

All data used to support the findings of this study are included within the article.

Conflicts of Interest

The authors declare that they have no conflicts of interest.

Authors' Contributions

Writing and original draft preparation were performed by Meng.K; writing, review, and editing were performed by Meng.K and Li.M.D; supervision and performance of the analysis with constructive discussions were carried out by Zhou.J. All authors have read and agreed to the published version of the manuscript.

Acknowledgments

The authors gratefully acknowledge Dalian Metro Line 5 Cross-sea Large Diameter Shield Construction project department for providing case data for this study and thanked the researchers and builders who provided help and support in the questionnaire survey. This research was funded by the Extreme Environmental Effects of Deep Sea Engineering Structures and Lifetime Service Safety Project (grant no. 2011CB013702).

References

[1] H. H. Einstein and S. G. Vick, "Geological model for tunnel cost model," in *Proceedings of the 2nd Rapid excavation and tunneling conference*, San Francisco, CA, USA, June 1974.

[2] H. H. Einstein, F. Chiabverio, and U. Koppel, "Risk analysis for alder tunnel," *Tunnels & Tunneling*, vol. 26, no. 11, pp. 28–30, 1994.

[3] H. H. Einstein, "Risk and risk analysis in rock engineering," *Tunnelling and Underground Space Technology*, vol. 11, no. 2, pp. 141–155, 1996.

[4] H. H. Einstein, "Geologic uncertainties in tunnelling," *Geotechnical Special Publication*, vol. 58, pp. 239–253, 2004.

[5] T. Isaksson, "Tunnelling in poor ground-choice of shield method based on reliability," in *Proceedings of the 11th Danube-European Conference on Soil Mechanics and Geotechnical Engineering*, Poreč, Croatia, May 1998.

[6] C. B. Chapman and M. Pinfold, "Design engineering - a need to rethink the solution using knowledge based engineering," in *Proceedings of the 18th SGES International Conference on Knowledge-Based Systems and Applied Artificial Intelligence*, Cambridge, England, December 1998.

[7] R. Sturk, L. Olsson, and J. Johansson, "Risk and decision analysis for large underground projects, as applied to the Stockholm Ring Road Tunnels," *Tunnelling and Underground Space Technology*, vol. 11, no. 2, pp. 157–164, 1996.

[8] T.: M. Q. Xian, "Development of the tunnel engineering in Japan and the statistics on the disaster," *Tunnel and Underground Engineering*, vol. 12, no. 4, pp. 1–9, 1998.

[9] S. Degn Eskesen, P. Tengborg, J. Kampmann, and T. Holst Veicherts, "Guidelines for tunnelling risk management: international tunnelling association, working group No.2," *Tunnelling and Underground Space Technology*, vol. 19, no. 3, pp. 217–237, 2004.

[10] H. Manchao, R. Leal e Sousa, A. Müller, E. Vargas r, L. Ribeiro e Sousa, and C. Xin, "Analysis of excessive deformations in tunnels forsafety evaluation," *Tunnelling and Underground Space Technology*, vol. 45, no. 1, pp. 190–202, 2015.

[11] K. C. Hyun, S. Min, H. Choi, J. Park, and I. M. Lee, "Risk analysis using fault-tree analysis (FTA) and analytic hierarchy process (AHP) applicable to shield TBM tunnels," *Tunnelling and Underground Space Technology*, vol. 49, no. 6, pp. 121–129, 2015.

[12] T. K. Nian, X. S. Guo, D. F. Zheng, Z. X. Xiu, and Z. B. Jiang, "Susceptibility assessment of regional submarine landslides triggered by seismic actions," *Applied Ocean Research*, vol. 93, Article ID 101964, 2019.

[13] X. S. Guo, D. F. Zheng, T. K. Nian, and L. T. Lv, "Large-scale seafloor stability evaluation of the northern continental slope of South China Sea," *Marine Georesources & Geotechnology*, vol. 38, no. 7, pp. 804–817, 2019.

[14] B. X. Yuan, M. Sun, L. Xiong, Q. Z. Luo, S. P. Pradhan, and H. Z. Li, "Investigation of 3D deformation of transparent soil around a laterally loaded pile based on a hydraulic gradient model test," *Journal of Building Engineering*, vol. 28, no. 3, Article ID 101024, 2020.

[15] H. Duddeck, "Challenges to tunnelling engineers," *Tunnelling and Underground Space Technology*, vol. 11, no. 1, pp. 5–10, 1996.

[16] E. Grov and O. T. Blindheim, "Risks in adjustable fixed price contracts," *Tunnels and Tunnelling International*, vol. 35, pp. 45–47, 2003.

[17] M. S. Wang, "Design construction and operation safety risk analysis of the Xiamen Submarine Tunnel," *Construction Technology*, vol. 1, pp. 7–10, 2005.

[18] J. M. Xiong, M. Hai, F. Huang, L. Xin, and Y. Xu, "Family cumulative risk and mental health in Chinese adolescents: the compensatory and moderating effects of psychological capital," *Psychological Development and Education*, vol. 36, no. 1, pp. 94–102, 2020.

[19] J. J. Chang, L. Yong, X. Xiao et al., "Combined use of food sweeteners in China and its cumulative risk assessment," *Journal of Toxicology*, vol. 35, no. 3, pp. 184–192, 2021.

[20] Y. Yuan, H. F. Wang, G. L. Ying, B. Zhang, and B. T. He, "Equal risk maintenance decision for power grid based on minimum cumulative risk," *Electric Power Automation Equipment*, vol. 37, no. 11, pp. 151–155, 2017.

[21] L. Zhang, Y. Q. Cheng, and Y. F. Xie, "An analysis on agricultural catastrophes and cumulative risks of crop insurance based on Copula —using crop insurance of Hunan province as an example," *Insurance Studies*, vol. 358, no. 2, pp. 65–71, 2018.

[22] World Health Organization, *Food Consumption and Exposure Assessment of Chemicals:Report of FAO/WHO Consulation on Food Consumption and Exposure Assessment of Chemicals*, World Health Organization, Geneva, Switzerland, 1997.

[23] Us Epa, *Proposed Guidance on Cumulative Risk Assessment of Pesticide Chemicals that Have a Common Mechanism of Toxicity*, United States Environmental Protection Agency, Washington DC, USA, 1997.

[24] G. W. Evans, D. Li, and S. S. Whipple, "Cumulative risk and child development," *Psychological Bulletin*, vol. 139, no. 6, pp. 1342–1396, 2013.

[25] G. Bankoff, G. Frerks, and D. Hilhorst, *Mapping Vulnerability, Disaster Development and People*, Earthscan Publishers, London, UK, 2004.

[26] Q. P. Wang, *System Dynamics*, Shanghai University of Finance & Economics Press, Shanghai, China, 2009.
[27] J. Assanee, B. A. Sorofman, Y. Sirisinsuk, and T. Kitisopee, "Factors influencing patient intention to report adverse drug reaction to community pharmacists: a structural equation modeling approach," *Research in Social and Administrative Pharmacy*, vol. 18, no. 4, pp. 2643–2650, 2022.
[28] J. F. Hair, B. Black, B. J. Babin, and R. Anderson, *Multivariate Data Analysis*, Machinery Industry Press, Beijing, China, 2011.
[29] A. T. Jebb, V. Ng, and L. Tay, "A review of key likert scale development advances: 1995-2019," *Frontiers in Psychology*, vol. 12, Article ID 637547, 2021.
[30] N. A. Dewi, L. S. R. Supriadi, and Y. Latief, "Development of WBS (Work Breakdown Structure) dictionary and checklist for safety planning of tunnel construction," in *Proceedings of the 3rd Tarumanagara International Conference of the Applications of Technology and Engineering (TICATE) 2020*, Jakarta, Indonesia, August 2020.
[31] H. J. Shyur, "A quantitative model for aviation safety risk assessment," *Computers & Industrial Engineering*, vol. 54, no. 1, pp. 34–44, 2008.
[32] Y. Wu, *Research on Conduction Mechanism and Control Mode of Rural Bank Credit Risk in China*, Doctor Thesis of Wuhan University of Technology, Hubei, China, 2014.
[33] L. Ma, G. M. Zhang, and P. Li, "Research on the transmission mechanism and transmission path of supply chain risk," *Journal of Library and Information Science*, vol. 17, no. 31, pp. 96–98, 2007.
[34] M. Barges, H. Cossette, and E. Marceau, "TVaR-based capital allocation with copulas," *Insurance: Mathematics and Economics*, vol. 45, no. 3, pp. 348–361, 2009.